Accepted Manuscript

The electrochemistry of 5-halocytosines at carbon based electrodes towards epigenetic sensing

I. Sanjuán, A.N. Martín-Gómez, J. Graham, N. Hernández-Ibáñez, C. Banks, T. Thiemann, J. Iniesta

PII: S0013-4686(18)31338-0

DOI: 10.1016/j.electacta.2018.06.050

Reference: EA 32043

To appear in: *Electrochimica Acta*

Received Date: 11 April 2018

Revised Date: 6 June 2018

Accepted Date: 7 June 2018

Please cite this article as: I. Sanjuán, A.N. Martín-Gómez, J. Graham, N. Hernández-Ibáñez, C. Banks, T. Thiemann, J. Iniesta, The electrochemistry of 5-halocytosines at carbon based electrodes towards epigenetic sensing, *Electrochimica Acta* (2018), doi: 10.1016/j.electacta.2018.06.050.

Graphical Abstract

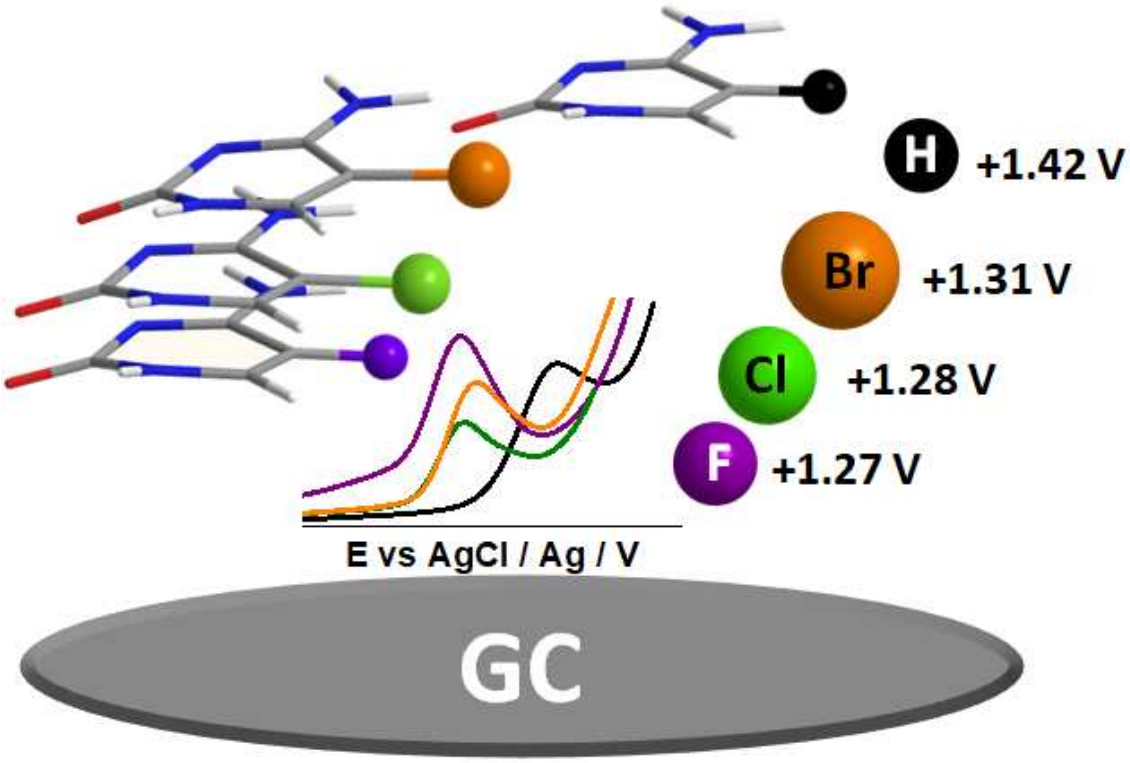

The electrochemistry of 5-halocytosines at carbon based electrodes towards epigenetic sensing

I. Sanjuán[1], A.N. Martín-Gómez[1], J. Graham[2], N. Hernández-Ibáñez[1], C. Banks[3], T. Thiemann[4], J. Iniesta[1]

[1] *Institute of Electrochemistry, Faculty of Science, Univ. Alicante, Alicante, 03080, Spain*

[2] *Galway-Mayo Institute of Technology, School of Science, Galway, Ireland*

[3] *Manchester Faculty of Science and Engineering, Manchester Metropolitan University, Chester Street, Manchester M1 5GD, UK*

[4] *Department of Chemistry, Faculty of Science, United Arab Emirates University, Al Ain, 15551, United Arab Emirates*

Submitted to: *Electrochimica Acta*

*Corresponding author: e-mail: jesus.iniesta@ua.es

Tel: +34 965909850

Fax: +34 965903537

Abstract

Epigenetic modifications in DNA are strongly linked to the triggering and development of pathophysiological disorders and cancer diseases. The halogenation of DNA via radical species, particularly the formation of 5-chlorocytosine (ClC), has recently emerged as epigenetic modification. This work deals for the first time with the exploration of the electrochemical behaviour of ClC on different carbon electrodes such as glassy carbon and boron-doped diamond using cyclic voltammetry and square wave voltammetry. When comparing both carbon materials, the use of glassy carbon turned out to be the appropriate in terms of a more well-defined anodic wave and higher sensitivity. The electrochemical oxidation potential of ClC resulted to be linearly dependent on the pH with a maximum current intensity in acetic acid buffer solution under the conditions used. Moreover, a linear response between peak current intensity and ClC concentration was obtained within the range of 200 and 1000 µM with a limit of detection of 200 µM. In order to elucidate the reaction mechanism of the process, the main oxidation products after a preparative electrolysis were detected by HPLC-MS. Simultaneous detection of ClC in the presence of the unmodified cytosine and mixtures containing other nucleic bases such as guanine, adenine and thymine was also addressed. Finally, the effect of the halogen atom (X=F, Cl, Br) located at position C-5 of the cytosine entity upon the electrooxidation process was examined by theoretical calculations, too.

Keywords: epigenetic modification, 5-chlorocytosine, 5-bromocytosine, glassy carbon, electrochemical sensor.

1. Introduction

Epigenetics is defined as the study of factors involved in the development of an organism, where gene expression plays an important role. The regulation of gene expression is mediated by reversible and highly selective DNA modifications that control the conformational transition of transcriptionally active or inactive DNA states. Many epigenetic mechanisms have already been discovered in a variety of physiological and pathological processes ranging from neurological [1], cardiovascular [2] and reproductive disorders [3] to several types of cancer diseases [4]. Nonetheless, epigenetic modifications are necessary for the development of living beings and are not always of a pathological nature. The problem arises when there are aberrant epigenetic patterns, which alter the normal expression of the genes. One type of aberrant epigenetic pattern already studied is the presence of methyl radicals in the DNA strands as a consequence of non-natural processes [5]. Methylation normally occurs in regions of the DNA sequence rich in cytosine and guanine residues called CpG islands, that consist of short DNA segments of about 300-3000 base pairs [4–6]. Naturally occurring methylation of the CpG islands within the selected genes in the DNA strand is an important epigenetic mechanism by which their expression can be silenced [2]. On the other hand, hypermethylation produces a fibrotic thickening that affects specific areas of the heart, giving rise to health problems [7].

Even though other aberrant epigenetic modifications may alter the natural gene expression such as the oxidation of guanine residues [8], the literature is still scarce about the consequences of nucleic base halogenation. In this regard, the presence of 5-halopyrimidines in DNA has been related to malfunctions of the recognition mechanism of certain restriction endonucleases [9], bringing about accelerated inflammation processes that are inherently mutagenic. Nevertheless, the fluorination of cytosine derivatives, i.e., to 5-fluoro-3-deoxycytidine (FdC), results in compounds that are inhibitors of the DNA methylation mechanisms early reported by Huber *et* al. [10], FdC being under study in clinical trials against breast cancer and other types of advanced developmental tumours [11]. Moreover, FdC has been shown to be able of binding and, at the same time, trapping DNA methyltransferases, thereby preventing DNA methylation [12,13]. With regard to chlorination of DNA bases, there exist few studies about the formation of 5-chlorocytosine (ClC) in DNA that could lead to the undesired

methylation of CpG islands, which is associated further with a deviant activation of tumour promoter genes or with the silencing of tumour suppressors [4,14].

For the aforementioned reasons, there is an incipient need to develop new analytical methodologies for selectively and specifically detecting such genetic aberrations in order to achieve a useful tool for an early detection of diseases. In this sense, during the last years, a plethora of techniques has been developed for the determination of this type of epigenetic modifications. In general, these methods consist of DNA extraction, followed by a subsequent protease and ribonuclease enzyme digestion step, which hydrolyses and separates the DNA strains into their constituent nucleic bases, to perform a final purification/separation step, using either HPLC methods [15] or electrophoretic techniques [16], both coupled with spectrometric detection. Even though the sensitivity and accuracy of such analytical techniques are high, the methodologies are usually tedious and cost-ineffective for routine analyses. An interesting alternative lies in the development of electrochemical sensors to obtain accurate and reproducible results along with a reduction in costs as well as better portability, miniaturization and the possibility of ex-situ and in-situ experiments. In this context, electrochemistry provides a potential tool, highly efficient and capable of solving drawbacks displayed by conventional techniques [17–20]. In addition, DNA is an electroactive macromolecule since the nucleic acids can be oxidised and reduced on various electrode materials [21,22].

Direct oxidation of DNA bases has been performed using a plethora of electrode materials such as mercury [23], platinum [24], gold [25], copper [26] and silver [27]. However, electrodes made of carbon materials are very interesting for the above purpose since they generally present higher electrochemical windows than the aforementioned metal-based materials and nucleic bases electrochemically react at high anodic potentials. The electrooxidation of nucleic bases, and more particularly, the electrooxidation of cytosine (C) and methylcytosine (mC) has been extensively reviewed in the literature [28]. For example, the electrooxidation of C and mC has been explored using glassy carbon (GC) [29], graphite (GPT) and screen printed graphite electrodes (SPGE) [30], boron doped diamond (BDD) [31,32], carbon nanotubes (CNT) [33] and graphene (GPH) [34].

To the best of our knowledge, no work has been published in the literature on the study of the electrochemical response of halocytosines, i.e., of 5-fluorocytosine (FC), 5-chlorocytosine ClC, and 5-bromocytosine (BrC) on carbon based electrodes,

which should elicit great interest for future application in the development of electrochemical sensors for epigenetic halogenated residues in DNA. In the present paper, for the first time the electrochemical behaviour of ClC at glassy carbon (GC), and boron doped diamond BDD has been compared by cyclic voltammetry (CV) and square wave voltammetry (SWV). The electrochemical behaviour of ClC has been studied in regard to pH, scan rate, ClC concentration and electrode surface pretreatment using GC electrode. The feasibility of ClC determination in the presence of cytosine (C) as well as other nucleic bases such as guanine (G), adenine (A), and thymine (T) has been addressed under optimised experimental conditions. A tentative reaction mechanism for the electrooxidation of ClC is also given, after an analysis of the products of a preparative electrolysis of ClC. Finally, the electrochemical response of FC, ClC and BrC has been explored in order to shed light on the influence of the halogen atom at 5-C position, and those results were examined by theoretical calculations.

2. Materials and methods

2.1. Reagents and chemicals

Free DNA bases [adenine (A), thymine (T), cytosine (C), guanine (G)] and 5-fluorocytosine (FC) of the highest purity were purchased (Sigma Aldrich). N-chlorosuccinimide (NCS, Sigma-Aldrich, 98 %), sodium carbonate (Fluka, analytical reagent grade) and liquid bromine (Sigma-Aldrich, 99 %) were purchased from Sigma Aldrich and used for the synthesis of the halocytosines 5-chlorocytosine (ClC) and 5-bromocytosine (BrC). Solutions were prepared with doubly distilled water, with a resistivity of not less than 18.2 MΩ cm. Nucleic base solutions were generally prepared in 0.1 M acetate / acetic acid buffer solution of pH 5.0 (sodium acetate, Scharlau Chemie S.A, 99% purity). Acetate buffer solutions were made up, setting pH values with glacial acetic acid (J. T. Backer, 99-100% purity) or NaOH (Scharlau Chemie S.A., reagent grade), and the pH measurements were carried out with a Crison Micro pH 2000 pH-meter. Guanine solution was prepared in 0.1 M acetate buffer solution of pH 5.0 up to saturated conditions, and then the solution was filtered through a 45 mm pore nylon filter (Millipore MILLEX-HN) in order to remove excess insoluble guanine. The final guanine concentration was determined by using a UV-visible spectrophotometer (UV-2401PC, Shimadzu) with an extinction coefficient of 10,700 cm^{-1} M^{-1} at λ = 243.0 nm, being always of 40 µM at saturated conditions [35]. Unless otherwise stated, the rest of

the nucleic bases tested in this work were dissolved in 0.1 M acetate buffer solution at pH 5.0.

2.2. Synthesis of ClC and BrC halocytosines

5-Chlorocytosine (ClC) and 5-bromocytosine (BrC), were synthesised as described in [36]. The synthesis consisted of the insertion of a halogen atom (Cl or Br) at the 5 position of the aromatic ring of the C moiety. Briefly, for ClC synthesis, 1.00 g of C (9 mmol) was dissolved in 20 mL of glacial acetic acid at 70 °C. Then, 1.32 g of NCS (9.9 mmol) was added dropwise over the course of 10 min. Thereafter, the mixture was maintained for 4 h at 70 °C, under reflux conditions and vigorous stirring. Thereafter, the reaction mixture was cooled down to room temperature to obtain a white precipitate. This precipitate was resuspended in 30 mL of ultrapure water and pH was set at 8.0 by the addition of solid sodium carbonate. The mixture was stirred again for 2-3 h and filtered off under vacuum. The final product was washed thoroughly several times with ultrapure water and subsequently dried overnight in an oven under vacuum.

For the synthesis of BrC, 2.5 g of C (22.5 mmol) were added to 37.5 mL of ultrapure water and then 1.15 mL of liquid bromine (22.5 mmol) was added dropwise to the mixture, keeping the temperature at 33°C. Afterwards, the reaction mixture was stirred at room temperature for 4 h and finally cooled down to 4 ºC overnight. Then, the precipitate was filtered off under vacuum to obtain colourless crystals, which thereafter were resuspended in 50 mL of ultrapure water. A total of 1.03 g of solid sodium carbonate was slowly added to the suspension. Finally, the suspension was left overnight under gentle stirring and subsequently filtered under vacuum. The final product was thoroughly washed with ultrapure water and dried in an oven at room temperature under vacuum for 3 h.

^{1}H and ^{13}C NMR spectroscopy were performed in order to check the purity of ClC and BrC: ^{1}H NMR of ClC (400 MHz, DMSO-d6): δ 7.09 (br s, 1H, NH) 7.60 (br s, 1H, NH), 7.71 (s, 1H, CH), 10.87 (br s, 1H, NH); ^{13}C (100 MHz, DMSO-d6) δ 98.3, 141.8, 155.7 and 162.6. ^{1}H NMR of BrC (400 MHz, DMSO-d6): δ 6.82 (br s, 1H, NH), 7.66 (br s, 1H, NH), 7.75 (s, 1H); ^{13}C (100 MHz, DMSO-d6) δ 85.6, 144.4, 155.9 and 163.2. The purity of ClC and BrC was evaluated by ^{1}H NMR spectroscopy to be higher than 95 %.

2.3. Electrochemical measurements

Electrochemical experiments were performed in a three-electrode standard electrochemical glass cell with a 10 mL volume. A glassy carbon (GC) bar with a 3 mm diameter (purity ≥ 99.95%, Goodfellow, UK), and a 3 mm diameter polycrystalline boron doped diamond (BDD) film mounted in polyether ether ketone [PEEK] doped with 0.1 wt.% of boron (Windsor Scientific Company, UK) were used as working electrodes (WE). The counter electrode (CE) was a gold wire, spirally wound, and the reference electrode (RE) was an AgCl/Ag electrode (1.0 M KCl), which was placed in a separate compartment via a luggin capillary. All the electrode potentials described in this work are always referred to this RE.

Cyclic Voltammetry (CV) and Square Wave Voltammetry (SWV) measurements were carried out using an Autolab PGSTAT 30 (Eco Chemie, The Netherlands) potentiostat/galvanostat and controlled by Autolab GPES software version 4.9 for Windows XP. All electrochemical experiments were carried out under a nitrogen atmosphere and set at 293 ± 2 K. SWV parameters used in all experiments were the following: modulation amplitude, 50 mV; frequency, 8 Hz; modulation step, 5 mV. SWV parameters were also optimised regarding the current intensity for the electrooxidation of halocytosines. Different frequencies were examined between 8 and 25 Hz, 8 Hz being the optimum frequency for an improved resolution of the voltammetric peaks.

GC and BDD electrodes were polished prior to the electrochemical measurements by using an alumina slurry suspension (Buehler, 0.3 mm particle size) with deionized water as lubricant, for 5 min. Then, the electrodes were thoroughly washed with deionized water and immersed into an ultrasonic cleaning bath (P-Selecta Ultrasons-H, 720 W output, 50 kHz) for 2 min for the removal of alumina residues adsorbed onto the carbonaceous surface. Both GC and BDD electrodes were dried under a nitrogen atmosphere prior to the electrochemical measurements.

The carbonaceous electrodes were also subjected to anodic and cathodic pre-treatments in order to investigate their effect on the electrochemical behaviour of ClC. The electrochemical pre-treatments consisted of performing 30 voltammetric sweeps in a 0.1 M acetate buffer solution at pH 5.0 between 0 and +2.5 V for the anodic pre-treatment and between 0 and -2.5 V for the cathodic pre-treatment [37]. Electrochemical pre-treatments were carried out in a separate electrochemical cell using a graphite bar as counter electrode and under stirring.

2.4. Preparative electrolysis

Preparative electrooxidation of ClC was performed using a two compartment H-shaped electrochemical cell separated by a Nafion 117 cationic exchange membrane (Dupont, France). A GC plate acted as the anode and a bipolar polycrystalline BDD electrode supported on silicon (from Adamant Technologies Switzerland of 2.5 x 4.0 cm) and doped with 700-800 ppm of boron acted as the cathode. The anodic compartment was filled with 50 mL of 1 mM ClC solution containing 0.1 M acetate buffer solution pH 5.0, while the cathodic compartment was filled with 50 mL of a 0.1 M acetate buffer solution pH 5.0. Electrolysis was carried out at a controlled potential of +1.4 V versus Ag/AgCl using a Potentiostat/ Galvanostat (AMEL Instruments Model 2049 General-Purpose Potentiometer) at room temperature under stirring and aerated conditions. The electrolysis was performed until the charge passed was 114 % of the theoretical charge, assuming an electron transfer of 2 electrons per mole of ClC. Both anodic and cathodic solutions were analysed after the electrolysis using a liquid chromatography-mass spectrometry system (LC/MS; Trap SL Agilent 1100) in order to determine the main products of the reaction. The mobile phase was made up of two components [A – water + 0.1% formic acid (JT Baker), and B – acetonitrile (HPLC grade Scharlau) + 0.1% acid formic (JT Baker)] with a 50:50 (v/v) in isocratic mode. A C18 commercial column of 250 mm x 4 mm with 5 mm particle size (Hyersil ODS) was used. An injection volume of 100 mL was always used for the samples of the electrolysed solution. The wavelength for detection was set at λ = 254 nm.

2.5. Computational calculations

All calculations were performed using Gaussian 09 rev. D01 [38]. Gas-phase structures were optimized using the B3LYP functional [39] and 6-311+G(d,p) basis set. For calculations involving solvation, all structures were reoptimized using the polarizable continuum model of solvation (with water as the solvent) at the B3LYP/6-311+G(d,p) level. All optimized structures were confirmed to be energy minima through vibrational frequency calculations. Solvation free energies were determined using the SMD method (solvation model based on density) [40].

2.6. Statistics

Equations for linear plots were obtained by the least squares method with the help of the spreadsheet application for calculus, Microsoft EXCEL 2010. Confidence

intervals of the slope and the intercept were obtained using the statistical value ‘‘t student’’ (for N-2 freedom degrees, where N is the number of standards solutions used) for a confidence level of 95 %. Limit of detection (LoD) and quantification (LoQ) were calculated as three and ten times the noise level, respectively.

3. Results and discussion.

3.1. Electrochemical behaviour of a ClC solution.

Figure 1 shows a comparative study of the electrochemical response of ClC performed at GC and BDD, exhibiting the CV and SWV behaviour of 1.0 mM ClC in 0.1 M acetate buffer solution at pH 5.0. For the CV measurements (Figures 1A), the peak potential associated with the electrooxidation of ClC is located at +1.34 V and +1.40 V for GC and BDD, respectively. Consecutive positive and negative scans provide a slight reduction in current intensity likely associated with a partial fouling of the electrode surface. The SWVs (Figure 1B) display that the peak potentials of the ClC are found at +1.28 V and +1.43 V for GC and BDD, respectively. With regard to the current intensity, the ClC electrooxidation gives rise to a peak current of 15 µA for the GC and 9 µA for the BDD after subtracting the background response, while in the SWVs the peak current obtained is ca. 14 µA for GC and 7 µA for the BDD, demonstrating a good reproducibility over both CV and SWV techniques, within the experimental error. Differences obtained in terms of peak potential and current intensity for both electrodes can be ascribed not only to the nature of the carbonaceous electrode, but also to the character of the surface chemistry of the electrode. The sluggish electrochemical process for the BDD electrode could be associated to the lower electrical conductivity of the electrode [41] but also to the functionalisation of the surface of the BDD itself [42]. Additionally, the anodic peaks obtained with the GC present a more resolved anodic wave than that obtained using BDD. Accordingly, to further explore the electrochemical response of ClC, the potential and current intensity dependence on the scan rate (v) was explored by CV using the GC electrode (see Figure ESI-1). Investigation of the plot of peak current intensity (I_p) versus scan rate (v) and versus square root of v revealed that there is a linear dependence of I_p with $v^{1/2}$ and therefore a linear dependence of $\log_{10} I_p$ with $\log_{10} v$ ($R^2 = 0.990$) with a slope value of 0.57, near to a theoretical value of 0.50, corresponding to a pure diffusion controlled

process [43]. Moreover, the dependence of the peak potential (E_p) on the scan rate is characteristic of an irreversible process.

Figure 2 depicts the pH dependence of the electrochemical oxidation of 1 mM ClC solution in 0.1 M acetate buffer over a pH range between 3.0 and 8.0. The acetic acid/acetate composition with an ionic strength of 0.1 M was used for all the measurements in order to avoid interferences due to different supporting electrolytes [29,44,45]. Results indicate that E_p value shifts to lower positive values with increasing pH. A general linear pH-dependence of E_p with a slope of 48 mV per pH unit is obtained as shown in Figure 2B within a pH range between 3 and 6, which is close to the theoretical Nernstian value of 59 mV per pH unit. This indicates that an equal amount of protons and electrons is involved for the electrooxidation process. Nevertheless, it is worth noting that from a pH value of around 6 upwards, a change of the slope of plot E_p vs pH takes place, as indicated with an arrow in Figure 2B. This could be attributed most likely to the second pKa_2 value of ClC. The pKa_1 of C itself is 4.5 according to the literature [46] and the electron-withdrawing effect of the Cl atom at C5 must change the acid/base character of the molecule, lowering its corresponding first pKa_1 to a value of below 3.5, since the pKa_1 values for bromocytosine and iodocytosine are close to 3.25 and 3.56 according to [46,47]. In terms of current intensity, Figure 2C shows that the highest peak currents are reached in the range of pH 4.00 - 5.00, ie., within the range of pH buffering capacity, exhibiting a maximum at ca. pH 4.5. In this sense, within the range of pH buffering capacity of the acetate buffer solution. pH 5.0 was chosen for its high current intensity output towards electroanalytical determination. The dependence of the current intensity on pH is quite similar to that shown for the unmodified C using the same buffer solution, as stated elsewhere [48]. The highest current intensity for the ClC electrooxidation is seen at slightly lower pH than in the case of C. This fact corresponds well to a more acidic character of the ClC moiety. The explanation is not as simple as it seems, since at pH values higher and lower than the one where highest current intensity is achieved, the current intensity is reduced describing a volcano-like tendency. This makes it unclear whether the electroactive species is protonated or unprotonated, leaving the explanation of the effect of the pH directed either to the reacting compound or the adsorptive properties of the carbon surface [49].

The oxygen functionalisation of the carbon electrode surface is a key parameter to improve the electrochemical response [50]. In an attempt to enhance the current

intensity associated with the ClC electrooxidation response, the electrochemical pre-treatment of the GC electrode was examined, using either anodic or cathodic pre-treatments, as described in the experimental section. Neither the mechanical nor the anodic pre-treatments were efficient enough to provide a clear SWV wave for the electrooxidation of 100 µM ClC in 0.1 M acetate buffer solution at pH 5.0 at such low concentration, while the cathodic pre-treatment remarkably improved the electrochemical response of the ClC with a current intensity of ca. 1.5 µA and a peak potential of +1.31 V (see Figure ESI-2). Therefore, a likely partial reduction of oxygenated functional groups on the GC surface could lead to an appropriate balance between the hydrophilic/hydrophobic character of the carbon surface. The results obtained in respect to the amelioration of the electrochemical response of ClC are in accordance with the effect of the halogen atom on the hydrophilic character of the moiety. As commented above, electronegative Cl atoms have an electron-withdrawing effect, making ClC more hydrophobic and therefore less soluble in water, thereby enhancing its interaction on a more hydrophobic carbon surfaces by participating dispersive forces in addition to interactive forces between π-electrons of the aromatic ring and π-electrons of the carbon surface [49,51].

3.2. Electroanalytical figures of merit.

Even though the cathodic pre-treatment has been proven to be advantageous to obtain higher anodic peak current intensities, mechanical pre-treatment was chosen for its simplicity and quickness of analysis. In this regard, Figure 3 depicts the SWV response of distinct standard solutions of ClC in 0.1 M acetate buffer solution at pH 5.0. Linearity was found between 200 µM and 1000 µM, but standard solutions below 200 did not show a clear anodic wave (*vide infra*). From data obtained from SWV, a linear calibration plot was obtained as shown in the inset figure of Figure 3, depicting peak current intensity (background subtracted) versus ClC concentration. The regression equation of the curve is as follows: I_p / µA = (0.013 ± 0.003) [ClC/ µM] + (0.8 ± 1.9) (r^2 = 0.968, n = 3) for ClC. To assess the repeatability of the method, three calibration plots were registered on the same day, obtaining a coefficient of variation (CoV) of 3.90%. The LoD was 200 µM and the LoQ was 675 µM (three and ten times the noise level, respectively).

The assessment of possible interferences which might alter the analysis is of vital importance for the applicability of an electrochemical sensor. The main interfering

substance in CpG islands, present in real samples, is obviously cytosine. Accordingly, the electrochemical response of a mixture of C and ClC was first addressed using a GC. Figure 4 shows the different SWV responses obtained for mixtures of a variable C concentration with increasing amounts of ClC. The electrochemical oxidation of C takes place at more positive potentials (+1.42 V vs AgCl/Ag) than that of ClC. Accordingly, ClC can be unambiguously detected in the presence of C since the anodic waves are separated by about 150 mV. Peak potentials of both C and ClC resulted to be unaltered, irrespective of the concentration of both bases. Moreover, an inspection of the plot ClC concentration versus current intensity depicted a sensitivity of 0.011 μA μM^{-1}, close to that presented in the absence of C (Figure 3). Thus, the presence of C does not alter or inhibit the electrooxidation of ClC. More interestingly, one would expect that the incorporation of an electronegative group such as a Cl atom at C-5 position of C moiety would mean a higher electronic retention and a more difficult removal of an electron, which means that electrooxidation should be hindered. Nevertheless, our results show a contrary behaviour, since ClC electrooxidation occurs at less negative potentials compared to C peak potential *(vide supra)*.

Next, we turned to the simultaneous determination of ClC in the presence of guanine (G), adenine (A) and thymine (T). Figure 5 displays the electrochemical response of a solution mixture of A (1.0 mM), T (1.0 mM) and G (33.0 μM) with different concentrations of ClC (between 74 μM and 193 μM) at a GC electrode. As expected, there is a noticeably difference in peak potential between the A, T and G nucleic bases, as reported elsewhere [52]. It is also worth noting that the electrooxidation of T under the above experimental conditions takes place at a peak potential of ca. +1.28 V, which is 10 mV lower than that for the ClC. The above results represent a serious disadvantage for the simultaneous detection of ClC in the presence of a complex mixture containing T nucleic bases. Additionally, an anodic electrochemical signal is not clearly noticed, until a concentration of ca. 200 μM is reached.

3.3. Mechanism of the electrooxidation of ClC.

The elucidation of the reaction mechanism of the ClC electrooxidation is vital to explain the differences observed in the electrochemical response of ClC and C. One would expect that the electrooxidation of ClC will follow the same steps as does C at a carbonaceous electrode, as reported in the literature by Brotons et al. [28]. In order to

get insights into the mechanism of the ClC electrooxidation, the final main products after a preparative electrolysis were determined by HPLC coupled to mass spectrometry (Figure ESI-3 and ESI-4). Figure 6 depicts the mechanism of the ClC electrooxidation. The first step is the abstraction of an electron to give rise to a radical cation. The radical cation must have different resonance forms and can evolve along two different reaction pathways via the participation of the solvent (H_2O) to incorporate oxygenated groups. In this regard, product 1 is the major oxygenated species formed through the release of the Cl atom. This species corresponds to a m/z of 126.1 [OH-C^+ – 1] observed in our experiment, and can be attributed to the formation of 5 (or 6)–hydroxycytosine. The presence of hydroquinone-like structures can be supported by the appearance of a pale, brownish colour during the electrooxidation [53]. The release of the Cl atom has also been observed in the electrooxidation of aromatic structures such as chlorophenol at GC electrode [54]. The other main peak observed in the mass spectrum displays a m/z of 176.1, and corresponds to a doubly hydroxylated ClC derivative [$(ClC+2O)^+$ - 1], and is most likely product 2, 5-chloro-6-hydroxy-4-(hydroxyamino)-3,4-dihydropyrimidin-2(1H)-one. A product derived from a mono-hydroxylation of the amino function at C4 has not been detected, perhaps because it quickly undergoes further electrooxidation to product 2.

The formation of a dimer species has also been detected with a m/z of 289.2 [$2ClC+2H^+$]. Three characteristic peaks (pattern of Cl isotope distribution) support the presence of two Cl atoms in the same molecule. A m/z of 350.1 is also detected with three characteristic peaks due to the distribution isotope pattern of two Cl atoms which could be assigned either to the subsequent electrooxidation of the dimer species or to other products coming from an electropolymerisation process, which would also be a typical side reaction in this kind of electrooxidation [55]. Unreacted ClC is still detected in the final anolyte solution, while neither the starting material ClC nor any of the products were observed in the catholyte solution.

3.4. Effect of the halogen atom on the electrochemical response.

The effect of the halogen atom upon the electrochemical response of halocytosines (FC, ClC and BrC) was investigated at GC electrode. In doing so, the SWVs of 1.0 mM solution of each halocytosine in 0.1 M acetate buffer at pH 5.0 were performed, exhibiting peak potentials at +1.27 V, +1.28 V and +1.31 V, with current intensities of ca. 20, 18 and 25 µA for FC, ClC and BrC, respectively (Figure 7). As can

be seen, peak potentials of FC and ClC are close to each other (within the experimental measurement errors ca. ± 10 mV), while the peak potential for BrC is centred at slightly more positive potentials. Remarkably, BrC is the only halocytosine tested whose electrooxidation exhibits an anodic shoulder at +1.50 V vs AgCl/Ag, most likely attributable to the electrooxidation of product/s derived from the BrC electrooxidation. The aforementioned behaviour cannot be explained by an increase in electronegativity of the halogen atom since the tendency of the electrooxidation peak potential would shift to more positive potentials due to the electron-withdrawing effect of F>Cl>Br atoms and the observed trend in the values of the peak potentials is exactly the opposite. In mechanistic terms, an additional resonance stabilisation of the radical cation intermediate by the lone electronic pair of the halogen atom could be used to help rationalize the observed trend, but this only would explain the higher oxidation potential of the C with respect to the halocytosines, but would not help to explain the trend among the halocytosines themselves.

In order to unravel this issue, theoretical calculations were developed based on the density functional theory to determine the differences observed for the electrooxidation of halocytosines. Table 1 compiles the calculated energies of the HOMO orbital of the halocytosine FC, ClC, BrC and the unmodified C. It would be expected from gas-phase HOMO energies that oxidation potentials would follow the trend ClC>FC>BrC>C, the opposite trend to that observed experimentally. On inclusion of solvation effects, the predicted trend is C>FC>ClC>BrC, and the above tendency could be explained by an additional resonance stabilisation by the lone pairs of the halogen atoms, but it does not fit with the observed experimental data, either.

Based on total free energy calculations, depicted in Table 2, it would be expected that the oxidation potentials would follow the trend BrC>ClC>C>FC. In this regard, the trends in free energy and solvation energy for the halogenated bases do correlate with the observed oxidation potentials, but the unsubstituted cytosine does not fit the pattern in this case. It appears that differences between the oxidation potentials of the halogenated bases can be explained primarily by changes in solvation energy upon oxidation, but the difference between the unmodified cytosine oxidation potential and the halocytosines cannot be explained in this way. The unsubstituted cytosine would be expected to be the most basic of the series: oxidation of the protonated form would be much more difficult and the calculated free energy change on oxidation would correlate well with the observed oxidation potentials with the non-protonated halogenated species

(see Figure ESI-5). However, this is controversial, because there should be both protonated and non-protonated cytosine at pH = 5 and, as already commented, we cannot assure that the protonated C is the electroactive specie reacting, although it would explain the behaviour.

It is possible that the remarked behaviour has to do additionally with the interaction of the compounds with the electrode surface, which has been discussed in a previous section. As already commented before, the electronegative halogen atoms present an electron-withdrawing effect and would make the compounds less hydrophilic and less soluble in water, enhancing their interaction on hydrophobic carbon surfaces. According to the electronegativity of the different halogen atoms and the expected hydrophilic character of C>BrC>ClC>FC, the trend in the observed oxidation potentials would be explained in this way, also.

3 Conclusions.

The CV and SWV response of ClC on glassy carbon electrode gave rise to an irreversible and diffusion controlled electrochemical oxidation peak, involving an overall equal number of protons and electrons exchanged. The electrooxidation of ClC showed a linear response of current intensity versus ClC concentration within the range 200-1000 μM with a limit of detection of 200 μM. The feasibility of simultaneous detection of ClC in the presence of other nucleic bases such as adenine, guanine, and thymine was also explored for the GC electrode, only showing an overlapping response with the thymine signal. The electrooxidation mechanism ClC goes through can be explained, with the products stemming mainly from both the hydroxylation of the ClC moiety with loss of the chloro atom and dimer formation derived from a ClC radical cation. As far as the effect of the halogen atom on the electrooxidation potential is concerned, the ClC anodic peak appears close to that of other halocytosines such as BrC or FC. Overall, the electrooxidation of the halogenated cytosines takes place at less positive potentials than the electrooxidation of cytosine itself.

Anodic potentials for the electrooxidation of halocytosines correlate well with data obtained from free energy and solvation energy theoretical calculations, but the electrochemical behaviour of the unsubstituted cytosine still remains unclear. The different electrochemical behaviour could be attributed to changes in the electronic density within the molecule through the effect of the halogen atom, which have a

relevant influence upon both the chemical properties of the molecules and the interaction between the molecules and the electrode surface.

This first approach to the electrochemical determination of the halogenation pattern in DNA (chlorination and bromination) related to epigenetic aberrations is seen as the first step to the development of electrochemical sensors for ClC and BrC within biological samples such as urine, blood or other complex fluids.

Acknowledgement

I.S.M., N.H.I. and J.I. thank the Ministerio de Economia y Competitividad MINECO, Spain for its financial support by the research projects CTQ2013-48280-C3-3-R and CTQ2016-76231-C2-2-R.

References

[1] Y.L. Weng, R. An, J. Shin, H. Song, G. li Ming, DNA Modifications and Neurological Disorders, Neurotherapeutics. 10 (2013) 556–567.

[2] H. Tao, J.-J. Yang, K.-H. Shi, Z.-Y. Deng, J. Li, DNA methylation in cardiac fibrosis: new advances and perspectives., Toxicology. 323 (2014) 125–9.

[3] S.J. Stocks, R.M. Agius, N. Cooley, K.L. Harrison, D.R. Brison, G. Horne, A. Gibbs, A.C. Povey, Alkylation of sperm DNA is associated with male factor infertility and a reduction in the proportion of oocytes fertilised during assisted reproduction., Mutat. Res. 698 (2010) 18–23.

[4] B.I. Fedeles, B.D. Freudenthal, E. Yau, V. Singh, S. Chang, D. Li, J.C. Delaney, S.M. Wilson, J.M. Essigmann, Intrinsic mutagenic properties of 5-chlorocytosine: A mechanistic connection between chronic inflammation and cancer, Proc. Natl. Acad. Sci. 112 (2015) E4571–E4580.

[5] M.T. Dyson, D. Roqueiro, D. Monsivais, C.M. Ercan, M.E. Pavone, D.C. Brooks, T. Kakinuma, M. Ono, N. Jafari, Y. Dai, S.E. Bulun, Genome-Wide DNA Methylation Analysis Predicts an Epigenetic Switch for GATA Factor Expression in Endometriosis, PLoS Genet. 10 (2014) e1004158.

[6] P. Haggarty, G. Hoad, G.W. Horgan, D.M. Campbell, M. Constancia, DNA Methyltransferase Candidate Polymorphisms, Imprinting Methylation, and Birth Outcome, PLoS One. 8 (2013) e68896.

[7] R. Neary, C.J. Watson, J.A. Baugh, Epigenetics and the overhealing wound: The role of DNA methylation in fibrosis, Fibrogenes. Tissue Repair. 8 (2015) 1–13.

[8] J. Cadet, J. Richard Wagner, DNA base damage by reactive oxygen species, oxidizing agents, and UV radiation, Cold Spring Harb. Perspect. Biol. 5 (2013)

[9] A. Olszewska, J. Dadová, M. Mačková, M. Hocek, Cleavage of DNA containing 5-fluorocytosine or 5-fluorouracil by type II restriction endonucleases, Bioorganic Med. Chem. 23 (2015) 6885–6890.

[10] B.E. Huber, E.A. Austin, C.A. Richards, S.T. Davist, S.S. Good, Metabolism of 5-fluorocytosine to 5-fluorouracil in human colorectal tumor cells transduced with the cytosine deaminase gene: Significant antitumor effects when only a small percentage of tumor cells express cytosine deaminase, Proc. Natl. Acad.

Sci. USA. 91 (1994) 8302–8306.
[11] J.H. Beumer, J.L. Eiseman, R.A. Parise, E. Joseph, J.L. Holleran, J.M. Covey, M. J. Egorin, Pharmacokinetics, Metabolism, and Oral Bioavailability of the DNA Methyltransferase Inhibitor 5-Fluoro-2′-Deoxycytidine in Mice, Clin. Cancer Res. 12 (2006) 7483-7491.
[12] D.J. Baker, G. Wuenschell, L. Xia, J. Termini, S.E. Bates, A.D. Riggs, T.R. O'Connor, Nucleotide excision repair eliminates unique DNA-protein cross-links from mammalian cells., J. Biol. Chem. 282 (2007) 22592–604.
[13] Q. Zhao, J. Fan, W. Hong, L. Li, M. Wu, Inhibition of cancer cell proliferation by 5-fluoro-2'-deoxycytidine, a DNA methylation inhibitor, through activation of DNA damage response pathway, Springerplus, 1 (2012), 65.
[14] V.V. Lao, J.L. Herring, C.H. Kim, A. Darwanto, U. Soto, L.C. Sowers, Incorporation of 5-chlorocytosine into mammalian DNA results in heritable gene silencing and altered cytosine methylation patterns, Carcinogenesis. 30 (2009) 886–893.
[15] K.L. Harrison, M. Wood, N.P. Lees, C.N. Hall, G.P. Margison, A.C. Povey, Development and Application of a Sensitive and Rapid Immunoassay for the Quantitation of N7-Methyldeoxyguanosine in DNA Samples, Chem. Res. Toxicol. 14 (2001) 295–301.
[16] D.K. Lloyd, A.M. Cypess, I.W. Wainer, Determination of cytosine-β-D-arabinoside in plasma using capillary electrophoresis, J. Chromatogr. B Biomed. Sci. Appl. 568 (1991) 117–124.
[17] P. Mehrotra, Biosensors and their applications - A review, J. Oral Biol. Craniofacial Res. 6 (2016) 153–159.
[18] J. Wang, DNA biosensors based on Peptide Nucleic Acid (PNA) recognition layers. A review.Biosens. Bioelectron. 13 (1998) 757–762.
[19] T. Laube, S.V. Kergaravat, S.N. Fabiano, S.R. Hernández, S. Alegret, M.I. Pividori, Magneto immunosensor for gliadin detection in gluten-free foodstuff: Towards food safety for celiac patients, Biosens. Bioelectron. 27 (2011) 46–52.
[20] M.C. Morris, Fluorescent biosensors — Probing protein kinase function in cancer and drug discovery, Biochim. Biophys. Acta - Proteins Proteomics. 1834 (2013) 1387–1395.
[21] E. Palek, M. Fojta, Peer Reviewed: Detecting DNA Hybridization and Damage, Anal. Chem. 73 (2001) 74 A-83 A.
[22] T. Hossain, G. Mahmudunnabi, M.K. Masud, M.N. Islam, L. Ooi, K. Konstantinov, M. S. A. Hossain, B. Martinac, G. Alici, N. T. Nguyen, M. J. A. Shiddiky, Electrochemical biosensing strategies for DNA methylation analysis, Biosens. Bioelectron. 94 (2017) 63–73.
[23] M. Fojta, Mercury electrodes in nucleic acid electrochemistry: Sensitive analytical tools and probes of DNA structure. A review, Collect. Czechoslov. Chem. Commun. 69 (2004) 715–747.
[24] S.J. Kwon, A.J. Bard, DNA analysis by application of Pt nanoparticle electrochemical amplification with single label response, J. Am. Chem. Soc. 134 (2012) 10777–10779.
[25] D.-W. Pang, Y.-P. Qi, Z.-L. Wang, J.-K. Cheng, J.-W. Wang, Electrochemical oxidation of DNA at a gold microelectrode, Electroanalysis. 7 (1995) 774–777.
[26] M.H. Ghanim, K. Hasan, N. Najimudin, M.Z. Abdullah, Design of DNA Biosensors and Amperometric Microchips Featuring Copper Electrodes, Proc. IEEE-EMBS Int. Conf. Biomed. Heal. Informatics. 25 (2012) 1005–1008.
[27] C. Fan, H. Song, X. Hu, G. Li, J. Zhu, X. Xu, D. Zhu, Voltammetric response

and determination of DNA with a silver electrode, Anal. Biochem. 271 (1999) 1–7.

[28] A. Brotons, F.J. Vidal-Iglesias, J. Solla-Gullón, J. Iniesta, Carbon materials for the electrooxidation of nucleobases, nucleosides and nucleotides toward cytosine methylation detection: a review, Anal. Methods. 8 (2016) 702–715.

[29] A.M. Oliveira-Brett, J.A.P. Piedade, L.A. Silva, V.C. Diculescu, Voltammetric determination of all DNA nucleotides, Anal. Biochem. 332 (2004) 321–329.

[30] A. Brotons, L.A. Mas, J.P. Metters, C.E. Banks, J. Iniesta, Voltammetric behaviour of free DNA bases, methylcytosine and oligonucleotides at disposable screen printed graphite electrode platforms., Analyst. 138 (2013) 5239–49.

[31] C. Deng, Y. Xia, C. Xiao, Z. Nie, M. Yang, S. Si, Electrochemical oxidation of purine and pyrimidine bases based on the boron-doped nanotubes modified electrode, Biosens. Bioelectron. 31 (2012) 469–74.

[32] L. Svorc, K. Kaldrer, Modification-free electrochemical approach for sensitive monitoring of purine DNA bases: Simultaneous determination of guanine and adenine in biological samples using boron-doped diamond electrode, Sens. Actuators, B. 194 (2014) 332-342.

[33] P. Wang, H. Chen, J. Tian, Z. Dai, X. Zou, Electrochemical evaluation of DNA methylation level based on the stoichiometric relationship between purine and pyrimidine bases, Biosens. Bioelectron. 45 (2013) 34–39.

[34] X. Zheng, L. Wang, Direct Electrocatalytic oxidation and simultaneous determination of 5-methylcytosine and cytosine at electrochemically reduced graphene modified glassy carbon electrode, Electroanalysis. 25 (2013) 1697–1705..

[35] G.D. Fasman, Handbook of biochemistry and molecular biology, CRC Press, 1975.

[36] J. Jansa, A. Lyčka, A. Růžička, M. Grepl, J. Vaněček, Synthesis, structure and rearrangement of iodinated imidazo[1,2-c]pyrimidine-5(6H)-ones derived from cytosine, Tetrahedron. 71 (2015) 27–36.

[37] T. A. Enache, A. Chiorcea-Paquim, O. Fatibello-Filho, A. M. Oliveira-Brett, Hydroxyl radicals electrochemically generated "in situ" on a boron-doped diamond electrode, Electrochem. Commun. 11 (2009), 1342-1345.

[38] Gaussian 09, Revision D01, M. J. Frisch, G. W. Trucks, H. B. Schlegel, G. E. Scuseria, M. A. Robb, J. R. Cheeseman, G. Scalmani, V. Barone, B. Mennucci, G. A. Petersson, H. Nakatsuji, M. Caricato, X. Li, H. P. Hratchian, A. F. Izmaylov, J. Bloino, G. Zheng, J. L. Sonnenberg, M. Hada, M. Ehara, K. Toyota, R. Fukuda, J. Hasegawa, M. Ishida, T. Nakajima, Y. Honda, O. Kitao, H. Nakai, T. Vreven, J. A. Montgomery, Jr., J. E. Peralta, F. Ogliaro, M. Bearpark, J. J. Heyd, E. Brothers, K. N. Kudin, V. N. Staroverov, R. Kobayashi, J. Normand, K. Raghavachari, A. Rendell, J. C. Burant, S. S. Iyengar, J. Tomasi, M. Cossi, N. Rega, J. M. Millam, M. Klene, J. E. Knox, J. B. Cross, V. Bakken, C. Adamo, J. Jaramillo, R. Gomperts, R. E. Stratmann, O. Yazyev, A. J. Austin, R. Cammi, C. Pomelli, J. W. Ochterski, R. L. Martin, K. Morokuma, V. G. Zakrzewski, G. A. Voth, P. Salvador, J. J. Dannenberg, S. Dapprich, A. D. Daniels, Ö. Farkas, J. B. Foresman, J. V. Ortiz, J. Cioslowski, and D. J. Fox, Gaussian, Inc., Wallingford CT, 2009.

[39] A.D. Becke, Density□functional thermochemistry. III. The role of exchange, J. Chem. Phys 98 (1993) 5648-5652.

[40] A. V. Marenich, C. J. Cramer, and D. G. Truhlar. Universal Solvation Model Based on Solute Electron Density and on a Continuum Model of the Solvent

Defined by the Bulk Dielectric Constant and Atomic Surface Tensions. J. Phys. Chem. B 113 (2009), 6378-6396

[41] R. Ramesham, T. Roppel, C. Ellis, B. Loo, Electrical Characterization of Undoped and Boron Doped Polycrystalline Diamond Thin Films, J. Electrochem. Soc. 138 (1991) 4–7.

[42] T.A. Ivandini, Y. Einaga, Polycrystalline boron-doped diamond electrodes for electrocatalytic and electrosynthetic applications, Chem. Commun. 53 (2017) 1338–1347.

[43] A.J. Bard, L.R. Faulkner, Electrochemical Methods: Fundamentals and Applications, Wiley, 2000.

[44] L. Jía, J. Liu, H.Wang, Electrochemical Performance and Detection of 8-hydroxy-2'-deoxyguanosine at single-stranded DNA Functionalized Graphene Modified Glassy Carbon Electrode, Biosens. Bioelectron. 67 (2015) 139-145.

[45] P. Wang, H. Wu, Z. Dai, X. Zou, Simultaneous Detection of Guanine, Adenine, Thymine and Cytosine at Choline Monolayer Supported Multiwalled Carbon Nanotubes Film, Biosens. Bioelectron. 26 (2010) 3339-3345.

[45] V. Verdolino, R. Cammi, B.H. Munk, H.B. Schlegel, Calculation of pKa Values of Nucleobases and the Guanine Oxidation Products Guanidinohydantoin and Spiroiminodihydantoin using Density Functional Theory and a Polarizable Continuum Model, J. Phys. Chem. B. 112 (2008) 16860–16873.

[46] D.G. Jacobson, F.A. Sedor, E.G. Sander, The Dehalogenation of Halocytosines by Bisulfite Buffers, Bioorg. Chem. 4 (1975) 72–83.

[47] V. Valinluck, W. Wu, P. Liu, J.W. Neidigh, L.C. Sowers, Impact of cytosine 5-halogens on the interaction of DNA with restriction endonucleases and methyltransferase, Chem. Res. Toxicol. 19 (2006) 556–562.

[48] C. Ruan, J. Lou, Y.-Y. Duan, W. Sun, Electrochemical Oxidation of Cytosine on Carbon Paste Electrode and Its Determination, J. Chinese Chem. Soc. 57 (2010) 1056–1060.

[49] C. Moreno-Castilla, Adsorption of organic molecules from aqueous solutions on carbon materials, Carbon 42 (2004) 83–94.

[50] I. Shpilevaya, J.S. Foord, Electrochemistry of methyl viologen and anthraquinonedisulfonate at diamond and diamond powder electrodes: The influence of surface chemistry, Electroanalysis 26 (2014) 2088–2099.

[51] M. Streat, J.W. Patrick, M.J. Camporro Perez, Sorption of Phenol and Para-Chlorophenol from water using conventional and novel activated carbons, Water Res. 29 (1995) 467–472.

[52] A.M. Oliveira Brett, F.-M. Matysik, Voltammetric and sonovoltammetric studies on the oxidation of thymine and cytosine at a glassy carbon electrode, J. Electroanal. Chem. 429 (1997) 95–99.

[53] X. Zhu, S. Shi, J. Wei, F. Lv, H. Zhao, J. Kong, Q. He, J. Ni, Electrochemical oxidation characteristics of p-substituted phenols using a boron-doped diamond electrode, Environ. Sci. Technol. 41 (2007) 6541–6546.

[54] P. Cañizares, J. Garcia-Gómez, M.A. Rodrigo, Electrochemical oxidation of several chlorophenols on diamond electrodes. Part 1. Reaction mechanism, J. Appl. Electrochem. 33 (2003) 917–927.

[55] I.P.G. Fernandes, B. V. Silva, B.N.M. Silva, A.C. Pinto, S.C.B. Oliveira, A.M. Oliveira-Brett, Isatin 1-morpholinomethyl, 1-hydroxymethyl, 1-methyl, and their halogenated derivatives, redox behaviour, J. Electroanal. Chem. 812 (2017) 143–152.

Tables

Table 1. Calculated HOMO energies for the C, FC, ClC and BrC moieties both in gas phase and solvation.

	HOMO gas phase /eV	HOMO (PCM H_2O) /eV
C	-6.665	-6.810
FC	-6.718	-6.786
ClC	-6.723	-6.764
BrC	-6.704	-6.729

Table 2. Total free energy calculations (PCM) for the oxidation and solvation of the C, ClC, BrC, FC and the protonated C (CH^+).

	ΔG oxidation (kJ/mole)	**ΔG Solvation (kJ/mole)**
C→C^+	145.26	-52.94
FC→FC^+	144.53	-53.55
ClC→ClC^+	145.78	-50.42
BrC→BrC^+	148.02	-46.85
CH^+→CH^{2+}	163.00	-158.26

Figures and Figures captions

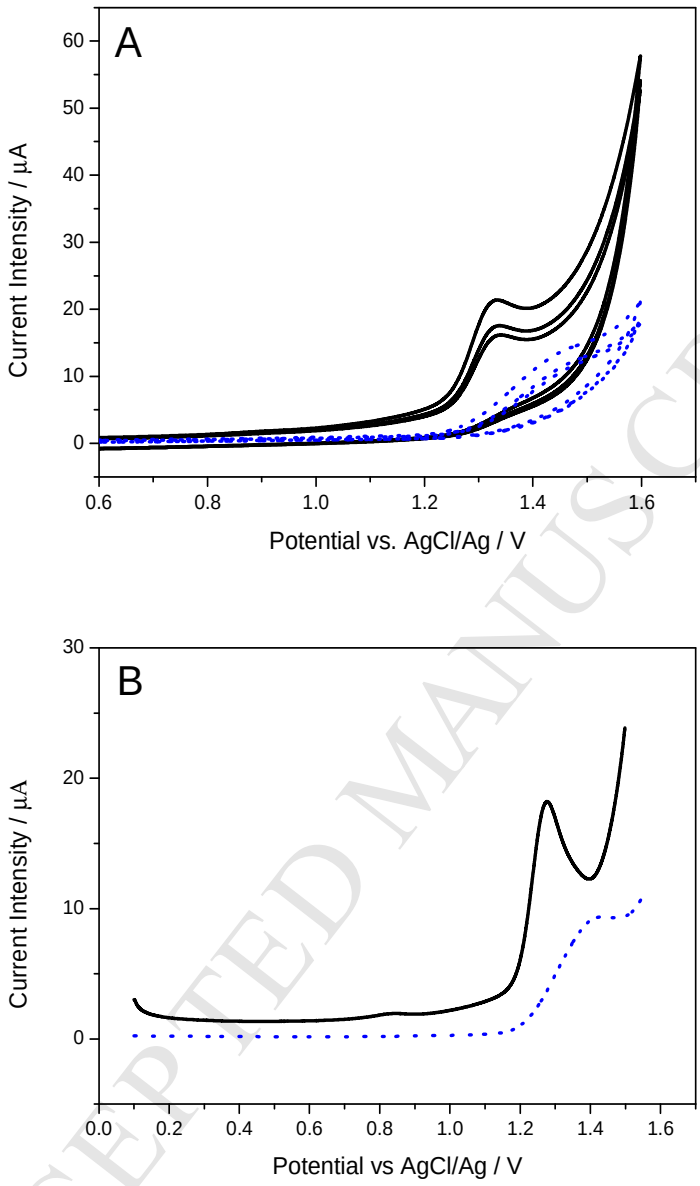

Figure 1. A) CV and B) SWV responses of 1.0 mM ClC in 0.1 M acetate buffer solution at pH 5.0 for GC (Black solid line), and BDD (Blue dotted line). CV parameters: Scan rate: 50 mV s^{-1}. Three consecutive scans. SWV parameters: modulation amplitude, 50 mV; frequency, 8 Hz; modulation step, 5 mV.

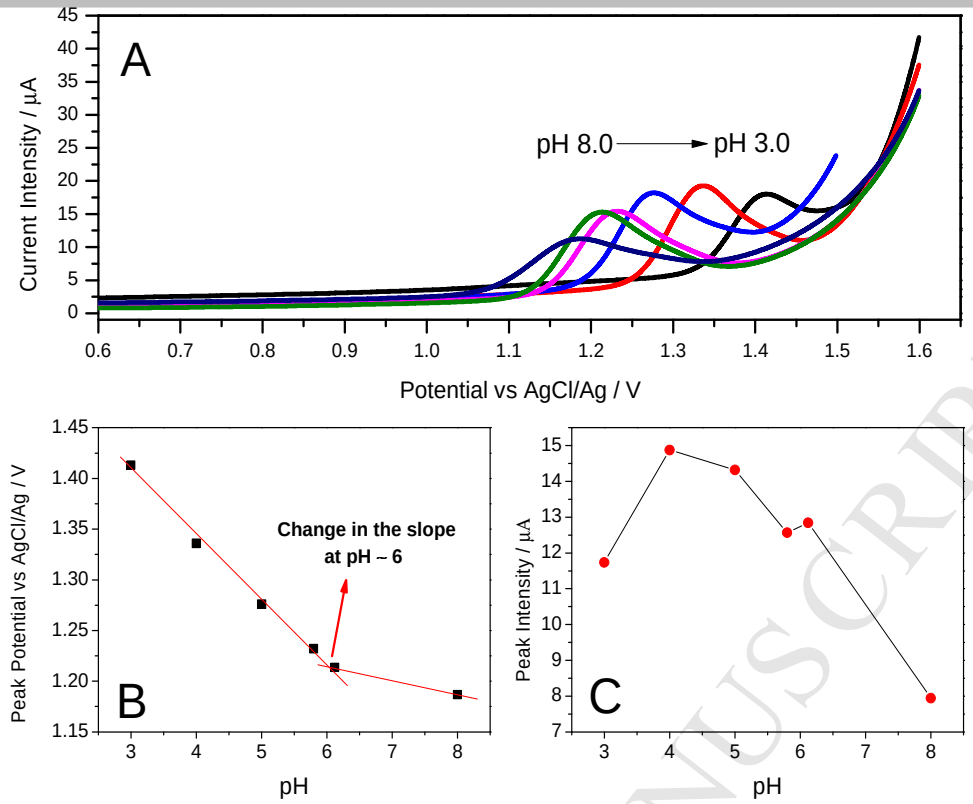

Figure 2. A) SWV responses of 1.0 mM ClC as a function of pH. 0.1 M acetate buffer solution adjusted at pH values between 3.0 and 8.0 (3.0, 4.0, 5.0, 5.8, 6.1, 8.0). B) Plot of peak potential versus pH. Red lines describe the two different trends of peak potential with pH. C) Plot of peak current intensity with pH. SWV parameters: modulation amplitude, 50 mV; frequency, 8 Hz; modulation step, 5 mV.

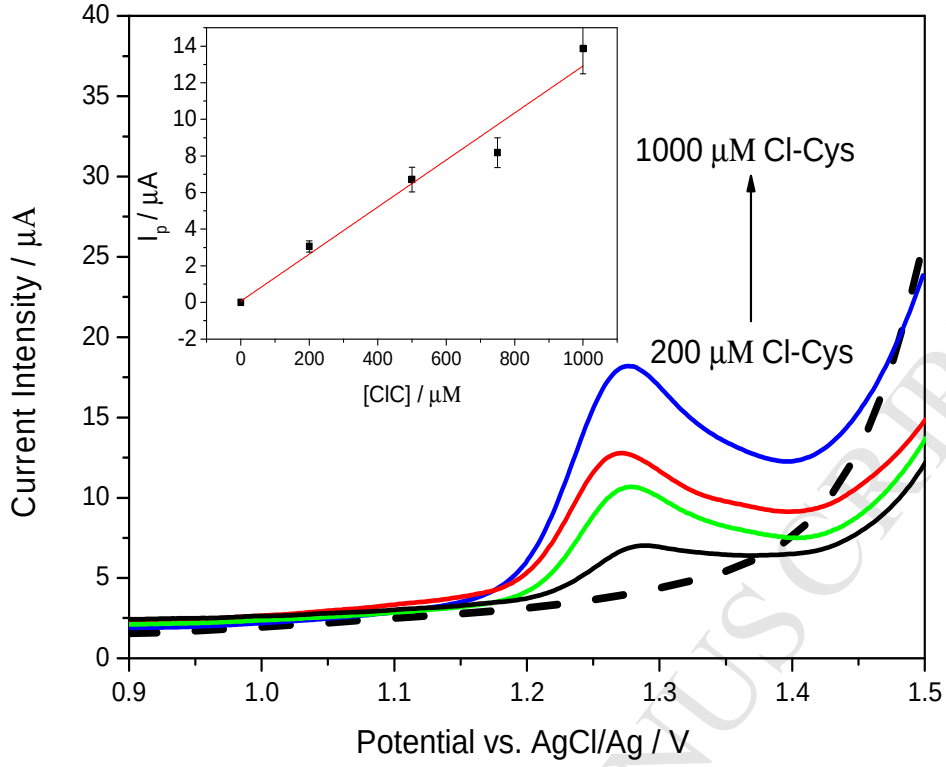

Figure 3. SWV responses of standard solutions of ClC (200, 500, 750, 1000 µM) in 0.1 M acetate buffer solution at pH 5.0. Figure inset shows the calibration plot of ClC standard solutions with concentration recorded between 200 and 1000 µM (Background subtracted). SWV parameters: modulation amplitude, 50 mV; frequency, 8 Hz; modulation step, 5 mV.

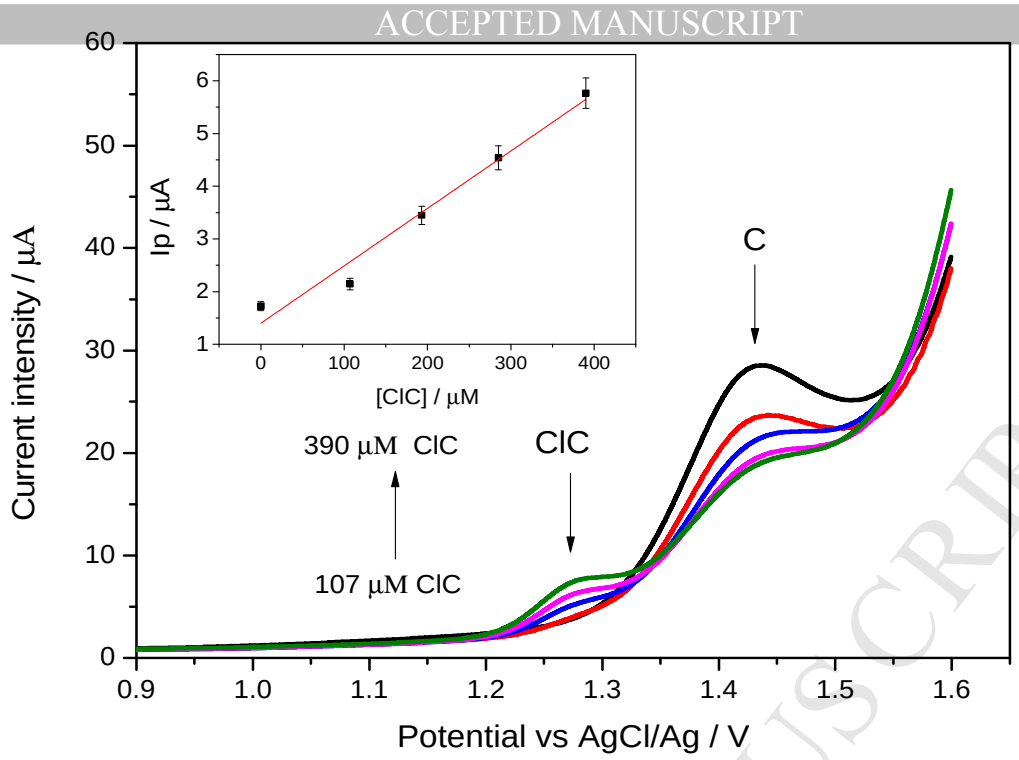

Figure 4. SWV responses of C plus ClC mixtures at different C to ClC ratios: 1000 µM C + 0 µM ClC (black line), 900 µM C + 107 µM ClC (red line), 850 µM C + 193 µM ClC (blue line), 800 µM C + 285 µM ClC (pink line) and 750 µM C + 390 µM ClC (green line). Mixtures in 0.1 M acetate buffer solution at pH 5.0. SWV parameters: modulation amplitude, 50 mV; frequency, 8 Hz; modulation step, 5 mV. **Inset figure.** Calibration plot of peak current (current subtracted) as a function of ClC concentration.

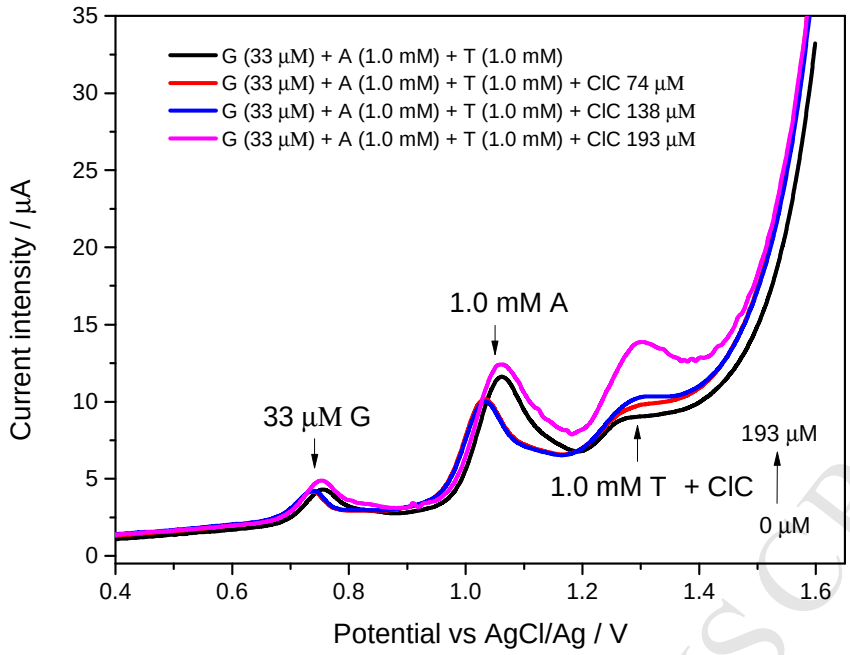

Figura 5. SWV responses of a mixture made of G (33 µM), A (1 mM), T (1 mM) with increasing amounts of ClC (0, 74, 138 and 193 µM) in 0.1 M acetate buffer solution at pH 5.0 using a GC electrode. SWV parameters: modulation amplitude, 50 mV; frequency, 8 Hz; modulation step, 5 mV.

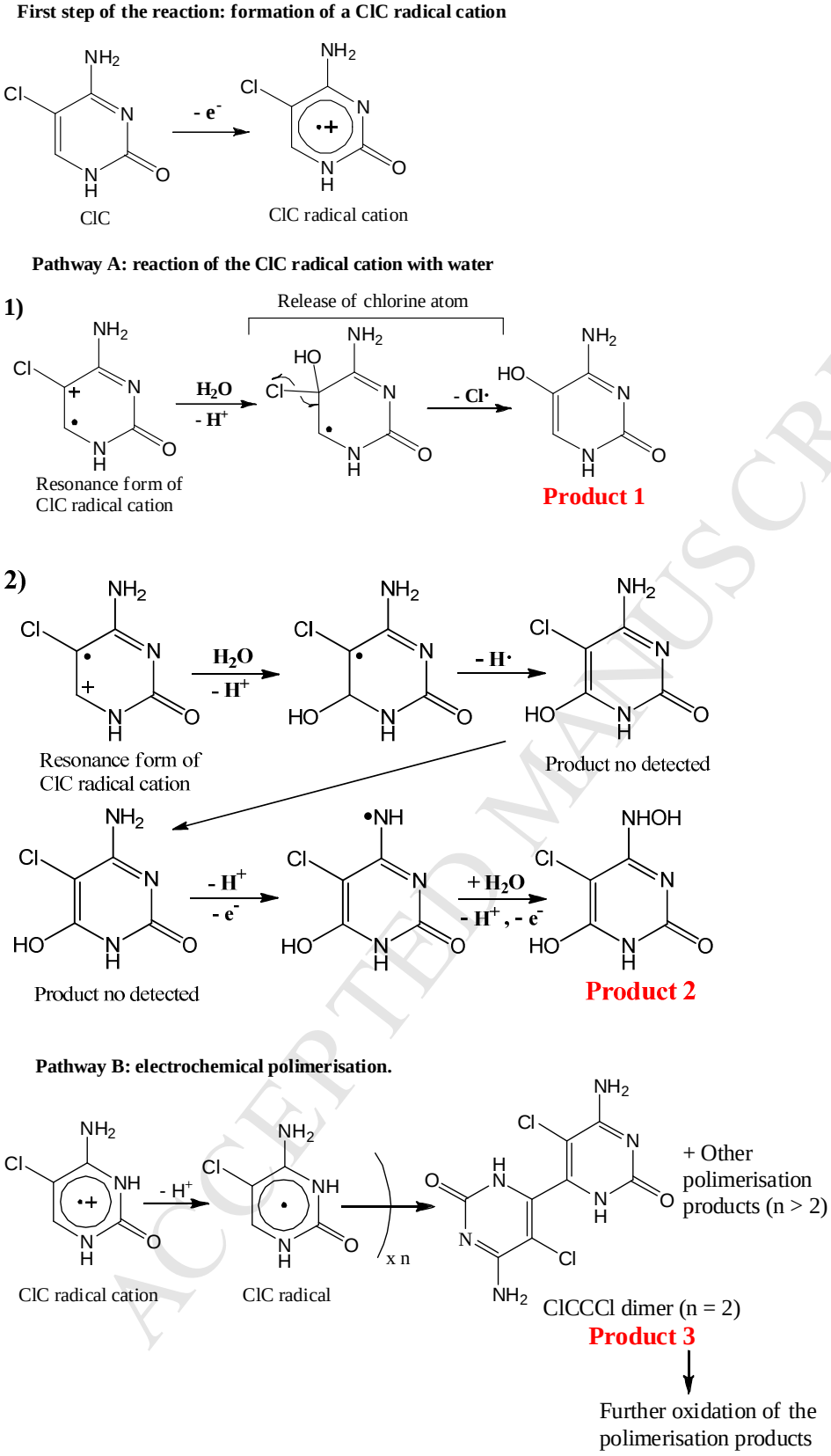

Figure 6. Scheme of the mechanism proposed for the electrochemical oxidation of the ClC at GC electrode.

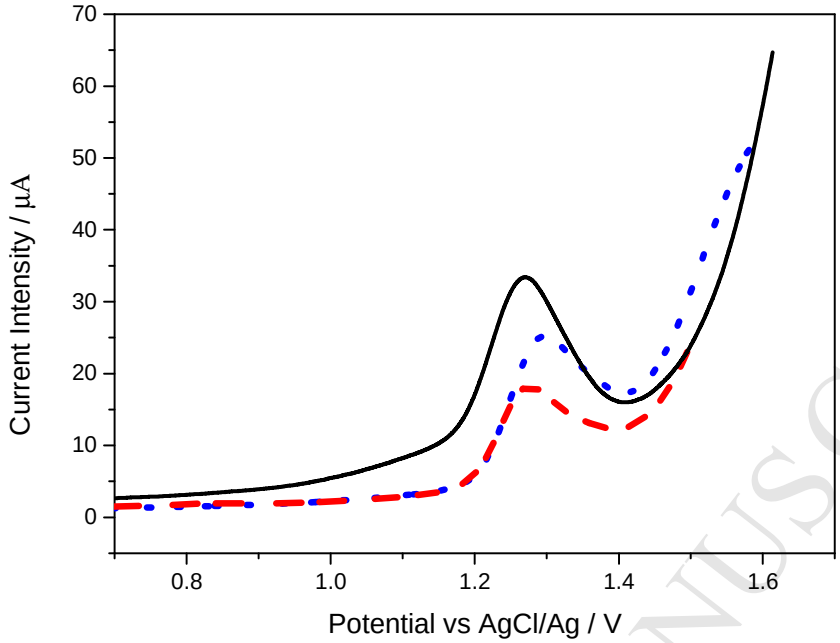

Figure 7. SWV responses of 1.0 mM FC (black solid line), 1.0 mM ClC (red dashed line) and 1.0 mM BrC (blue dotted line) in 0.1 M acetate buffer at pH 5.0 using a GC electrode. SWV parameters: modulation amplitude, 50 mV; frequency, 8 Hz; modulation step, 5 mV.

Highlights

- The electrochemical characterisation of chlorocytosine has been performed for the first time on glassy carbon electrode.
- Chlorocytosine can be electrochemically detected in the presence of other nucleobases.
- A mechanism reaction for the electrooxidation of chlorocytosine has been proposed.
- Free energy and solvation energy theoretical calculations of halocytosines agree with the electrooxidation peak potentials experimentally.
- Feasibility for an electrochemical sensor for the halogenation degree detection in DNA.